International Journal of Innovative
Computing, Information and Control
Volume 8, Number 5(A), May 2012

ICIC International ©2012 ISSN 1349-4198
pp. 3015–3028

SWITCHING T-S FUZZY MODEL-BASED GUARANTEED COST CONTROL FOR TWO-WHEELED MOBILE ROBOTS

Chung-Hsun Sun, Yin-Tien Wang and Cheng-Chung Chang

Department of Mechanical and Electro-mechanical Engineering
Tamkang University
No. 151, Yingzhuan Road, Tamsui District, New Taipei City 25137, Taiwan
chsun@mail.tku.edu.tw

Received January 2011; revised July 2011

Abstract. *Based on the switching Takagi-Sugeno (T-S) fuzzy control theorem, this study investigates the position control for a developed differential-drive two-wheeled mobile robot (TWMR). The developed TWMR is introduced, followed by a description of the kinematic equations of the TWMR, which are represented by exact T-S fuzzy systems. The uncontrollable problem of the derived T-S fuzzy model is avoided by considering the switching section mechanism. The switching T-S fuzzy model is synthesized by a switching parallel distributed compensation. Moreover, a guaranteed cost control issue is considered to obtain proper control signals and improve state responses for the developed TWMR. A feasible controller is obtained by solving the derived linear matrix inequalities (LMIs). Finally, the proposed control law is implemented on the developed TWMR, demonstrating the effectiveness of the control design.*

Keywords: Two-wheeled mobile robot, Switching T-S fuzzy system, Guaranteed cost control

1. **Introduction.** Mobile robots have received considerable attention for academic and industrial applications, including such as security, home services, medical care, industrial manufacturing, transportation and business services. Wheeled mobile robots are characterized by their ability to move rapidly on flat surfaces. Therefore, this work investigates the position control in a differential-drive two-wheeled mobile robot (TWMR). Nonlinear controller design for TWMR has been extensively studied [1-8]. Recent efforts have attempted to control TWMR by using fuzzy control [9-14].

As an effective and simple control method, linguistic fuzzy control is often designed based on the experience of designers without considering the system model. However, the stability of a traditional linguistic fuzzy control system cannot be guaranteed by mathematical analysis. T-S fuzzy control is a reliable scheme to ensure the stability of a system. T-S fuzzy model-based control has been extensively explored in recent decades [15]. Tanaka and Sugeno verified the stability of a T-S fuzzy system by using a quadratic Lyapunov function $V(k) = \mathbf{X}^T(k)\mathbf{P}\mathbf{X}(k)$ [15]. System stability is guaranteed if a common positive definite matrix $\mathbf{P}$ can satisfy the Lyapunov inequalities with respect to the T-S fuzzy system. Lyapunov inequalities can be converted into linear matrix inequalities (LMIs), and then be solved efficiently by LMI tools. Parallel distributed compensation (PDC) is conventionally adopted control design for T-S fuzzy model-based stabilization. The corresponding Lyapunov inequalities for PDC design can also be converted into LMIs. LMI-based fuzzy control design and common matrix $\mathbf{P}$ can be solved simultaneously by LMI tools. Hence, LMI-based T-S fuzzy control is applied to numerous applications, such as inverted pendulum, truck, overhead crane, networks and TWMR [15-21].

Despite the considerable attention paid to TWMR tracking control [9-14], position control of TWMR based on T-S fuzzy model is still problematic. By a sector nonlinearity method [15], the TWMR model can be converted to a T-S fuzzy model. However, the T-S fuzzy model for TWMR leads to an uncontrollable situation [16]. The uncontrollable issue can be avoided by using the switching T-S fuzzy model instead of the traditional T-S fuzzy model. This work adopts the switching T-S fuzzy modelling method to represent the kinematic equations of a differential-drive TWMR.

To apply PDC to a switching T-S fuzzy system, a switching PDC form should replace the traditional PDC. Stability of the switching T-S fuzzy control system is then proven using Lyapunov stability criterion. The derived Lyapunov inequalities are converted into LMIs, and solved by existing LMI tools as well. However, simulation results indicate that the control gains are too large for a practical TWMR system. In addition, simulation results demonstrate slow state responses. This work attempts to obtain better state responses and obtain proper control gains by using guaranteed cost control law. A control system should not only be asymptotically stable, but also guarantee a proper performance, which is referred to guaranteed cost control [22]. The performance constraint is represented by a cost function $J = \sum_k \mathbf{X}^T(k)\mathbf{W}\mathbf{X}(k) + \mathbf{u}^T(k)\mathbf{R}\mathbf{u}(k)$, where $\mathbf{W}$ and $\mathbf{R}$ denote given matrices corresponding to the state vector $\mathbf{X}(k)$ and input vector $\mathbf{u}(k)$, respectively. Better state responses can be obtained by selecting a proper matrix $\mathbf{W}$. The proper control gains can be achieved by choosing a proper matrix $\mathbf{R}$. Therefore, this work considers the guaranteed cost control law.

This study focuses on the switching T-S fuzzy model-based guaranteed control design for the developed TWMR. Kinematic equations of the differential-drive TWMR are represented as a switching T-S fuzzy model. Control design for the TWMR model is based on the guaranteed cost control law. Both the stability and reasonable control gain are guaranteed. The control law can be presented as LMIs and then effectively solved by MATLAB LMI tool. Finally, the control design is implemented on the developed TWMR. Experimental results demonstrate the effectiveness of the proposed control design.

2. System Description and Problem Formulation.

This section introduces the developed TWMR and its kinematics. Kinematics of the TWMR is then represented by T-S fuzzy model, followed by formulation of the derivative modelling problem.

2.1. Developed TWMR.

The developed TWMR measures $42 \times 49 \times 50$cm. The TWMR mechanism includes a vehicle body, two driving wheels and a passive caster, as shown in Figure 1. Figure 2 shows the overall control architecture of TWMR. According to the proposed switching T-S fuzzy model-based control law, the speed control command can be calculated using the PC-based controller. For safety considerations, speed command is transferred to a current command by a constant ratio $k^* = 1$. The current control avoids the current suddenly and hugely increasing while TWMR demands a large torque. An additional microcontroller, PIC18F4431 (Microchip Tech. Inc.), implements the current control. The built-in pulse width modulation (PWM) module of the PIC18F4431 can provide the current control signal for the driver circuit of the motor. Thus, two servo motors (CSDC-60) can actuate the two wheels of TWMR individually. Two 500 PPR (pulses per revolution) incremental encoders are attached to motors individually. The encoder feedback transmits to the PC-based controller through PIC18F4431 and FT232RL, where FT232RL is a converter for RS232 and USB. The control demand for TWMR is then achieved. The control law is addressed later.

2.2. Traditional T-S fuzzy model.

The differential-drive TWMR model and its coordinate system are shown in Figure 3. The variables are defined as follows. v_l and v_r are

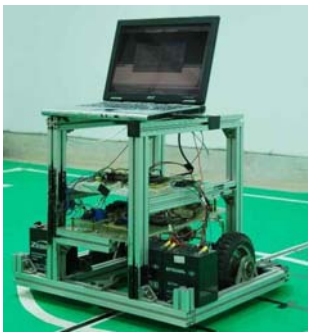

FIGURE 1. Photograph of the differential-drive TWMR

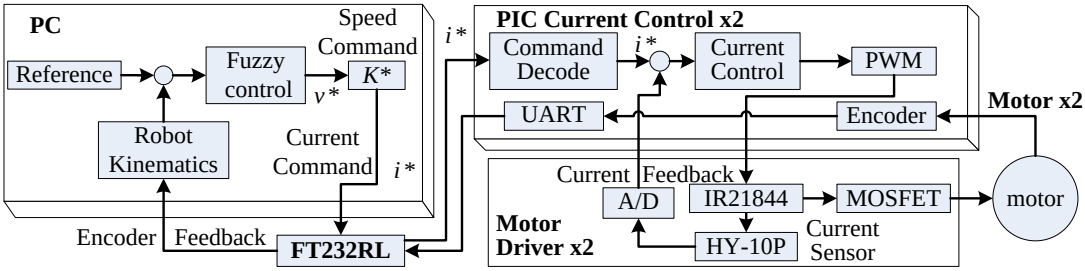

FIGURE 2. Control architecture of the developed TWMR

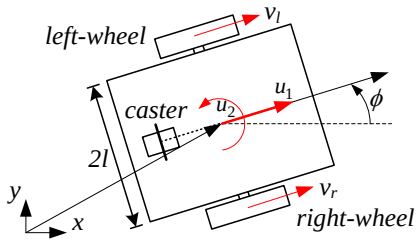

FIGURE 3. TWMR model and its coordinate system

the forward speeds of the left and right wheel, respectively. u_1 refers to the linear speed of the robot. u_2 refers to the angular velocity of the robot. ϕ is the orientation angle of the robot. l denotes the half width of the robot. Therefore, the kinematic equations of the TWMR are presented as follows:

$$x(k+1) = x(k) + [(v_r + v_l)\Delta t \cdot \cos\phi(k)]/2 \tag{1}$$

$$y(k+1) = y(k) + [(v_r + v_l)\Delta t \cdot \sin\phi(k)]/2 \tag{2}$$

$$\phi(k+1) = \phi(k) + [(v_r - v_l)\Delta t]/(2l) \tag{3}$$

where Δt is the sampling time. For a differential-drive TWMR, we define

$$u_1 = (v_r + v_l)/2 \tag{4}$$

$$u_2 = (v_r - v_l)/2 \tag{5}$$

Herein, the control purpose is $\lim_{k\to\infty} y(k) = 0$ and $\lim_{k\to\infty} \phi(k) = 0$. Therefore, the control object is described as

$$\begin{bmatrix} y(k+1) \\ \phi(k+1) \end{bmatrix} = \begin{bmatrix} 1 & 0 \\ 0 & 1 \end{bmatrix} \begin{bmatrix} y(k) \\ \phi(k) \end{bmatrix} + \begin{bmatrix} \sin\phi(k) & 0 \\ 0 & 1 \end{bmatrix} \begin{bmatrix} u_1(k) \\ u_2(k) \end{bmatrix} \Delta t \tag{6}$$

By using sector nonlinearity method [15] to replace the nonlinear term $\sin\phi(k)$ in (6), the T-S fuzzy model of TWMR is derived with the following procedures. Considering $\phi(k) \in [-3.131 \;\; 3.131]$ (i.e., $|\phi(k)| \leq 0.996\pi$), the maximum and minimum of $\sin\phi(k)$ are

$$\overline{b}_1 \equiv \min_{|\phi(k)\leq 0.996\pi|} \sin\phi(k) = -1, \quad \overline{b}_2 \equiv \max_{|\phi(k)\leq 0.996\pi|} \sin\phi(k) = 1 \tag{7}$$

According to the sector nonlinearity method, $\sin\phi(k)$ can be expressed as

$$\sin\phi(k) = M_1(\sin\phi(k)) \times \overline{b}_1 + M_2(\sin\phi(k)) \times \overline{b}_2 \tag{8}$$

where

$$M_1(\sin\phi(k)) = \frac{1-\sin\phi(k)}{\overline{b}_2 - \overline{b}_1}, \quad M_2(\sin\phi(k)) = \frac{\sin\phi(k) - (-1)}{\overline{b}_2 - \overline{b}_1} \tag{9}$$

$$M_1(\sin\phi(k)) + M_2(\sin\phi(k)) = 1 \tag{10}$$

Hence, (6) can be represented as a T-S fuzzy model composed of a set of linear subsystems,

Plant rule i: If $\sin\phi(k)$ is $M_i(\sin\phi(k))$, then $\mathbf{X}(k+1) = \mathbf{A}_i\mathbf{X}(k) + \mathbf{B}_i\mathbf{u}(k)$

where $i = 1, 2$, $\mathbf{A}_1 = \mathbf{A}_2 = \begin{bmatrix} 1 & 0 \\ 0 & 1 \end{bmatrix}$, $\mathbf{B}_1 = \begin{bmatrix} 1 & 0 \\ 0 & 1 \end{bmatrix} \Delta t$, $\mathbf{B}_2 = \begin{bmatrix} -1 & 0 \\ 0 & 1 \end{bmatrix} \Delta t$. The T-S fuzzy model of the TWMR is then expressed as

$$\mathbf{X}(k+1) = \sum_{i=1}^{2} w_i(k)[\mathbf{A}_i\mathbf{X}(k) + \mathbf{B}_i\mathbf{u}(k)] \tag{11}$$

where $\mathbf{X}(k) = [y(k) \;\; \phi(k)]^T$ and $\mathbf{u}(k) = [u_1(k) \;\; u_2(k)]^T$ denote the state vector and the input vector, respectively. And

$$w_i(k) = \frac{M_i(\sin\phi(k))}{\sum_{i=1}^{2} M_i(\sin\phi(k))} \tag{12}$$

Notably, in (11), a situation in which $\sin(\phi(k)) = 0$ leads to

$$\sum_{i=1}^{2} M_i(\sin\phi(k))\mathbf{B}_i\mathbf{u}(k) = \begin{bmatrix} 0 & 0 \\ 0 & 1 \end{bmatrix} \Delta t \cdot \mathbf{u}(k) \tag{13}$$

Then, the system is uncontrollable. Previous works [16,23] have presented similar results. To overcome the uncontrollable problem, the traditional T-S fuzzy model is replaced using the switching T-S fuzzy model.

2.3. **Switching T-S fuzzy model.** A traditional T-S fuzzy model and a switching T-S fuzzy model differ in the structure of non-overlapping region rules. The crisp region rules make the T-S fuzzy model with the utility of a switch system. In each region, a switching T-S fuzzy model is still composed of fuzzy rules, and it maintains the modelling superiority of a T-S fuzzy system. Notably, the crisp ranges of region rules must be defined in advance to represent the TWMR by the switching T-S fuzzy model [15,16].

Next, consider modelling $\sin\phi(k)$ by switching T-S fuzzy model in the following non-overlapping regions $\pi/50 < \phi(k) \leq 3.131$, $-\pi/50 \leq \phi(k) \leq (\pi/50)$ and $-3.131 \leq \phi(k) < -\pi/50$. The three regions are denoted as $\mathbf{S}_1$, $\mathbf{S}_2$ and $\mathbf{S}_3$, respectively. Figure 4 shows the division of $\sin\phi(k)$. In Region 1 ($\mathbf{S}_1$) and Region 3 ($\mathbf{S}_3$), the modelling procedures resemble (7)-(10). Due to the maximum and minimum of $\sin\phi(k)$ in $\mathbf{S}_1$ are

$$b_{11} \equiv \min_{\pi/50<\phi(k)\leq 3.131} \sin\phi(k) = 0.01, \quad b_{12} \equiv \max_{\pi/50<\phi(k)\leq 3.131} \sin\phi(k) = 1 \tag{14}$$

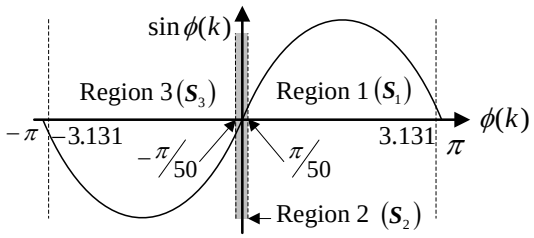

FIGURE 4. Division of the TWMR model

where $\sin\phi(k) \equiv z_1(k) \in [b_{11} \quad b_{12}]$ in $\mathbf{S}_1$. According to the sector nonlinearity method, $\sin\phi(k)$ in $\mathbf{S}_1$ can be represented as

$$\sin\phi(k) = \sum_{i=1}^{2} M_{1i}(z_1(k)) \cdot b_{1i} \tag{15}$$

where

$$M_{11}(z_1(k)) = \frac{1 - z_1(k)}{1 - (0.01)}, \quad M_{12}(z_1(k)) = \frac{z_1(k) - (0.01)}{1 - (0.01)} \tag{16}$$

Likewise, $\sin\phi(k) \equiv z_3$ in $\mathbf{S}_3$ can be represented as

$$\sin\phi(k) = \sum_{i=1}^{2} M_{3i}(z_3(k)) \cdot b_{3i} \tag{17}$$

where

$$b_{31} \equiv \min_{-3.131 \le \phi(k) < -\pi/50} \sin\phi(k) = -1, \qquad b_{32} \equiv \max_{-3.131 \le \phi(k) < -\pi/50} \sin\phi(k) = -0.01 \tag{18}$$

$$M_{31}(z_3(k)) = \frac{b_{32} - z_3(k)}{b_{32} - b_{31}}, \qquad M_{32}(z_3(k)) = \frac{z_3(k) - b_{31}}{b_{32} - b_{31}} \tag{19}$$

In $\mathbf{S}_2$, however, to avoid an uncontrollable circumstance (13), u_1 is set as a constant C. Then (6) can be expressed as

$$\begin{bmatrix} y(k+1) \\ \phi(k+1) \end{bmatrix} = \begin{bmatrix} 1 & C \cdot \frac{\sin\phi(k)}{\phi(k)} \cdot \Delta t \\ 0 & 1 \end{bmatrix} \begin{bmatrix} y(k) \\ \phi(k) \end{bmatrix} + \begin{bmatrix} 0 \\ 1 \end{bmatrix} u_2(k)\Delta t \tag{20}$$

Using sector nonlinearity method to replace the nonlinear term $\sin(\phi(k))/\phi(k) \equiv z_2$, allows us to obtain

$$\frac{\sin\phi(k)}{\phi(k)} = \sum_{i=1}^{2} M_{2i}(z_2(k)) \cdot a_{2i} \tag{21}$$

where

$$a_{21} = \min_{-\pi/50 \le \phi(k) \le \pi/50} \frac{\sin\phi(k)}{\phi(k)} = \frac{\sin(\pi/50)}{\pi/50}, \qquad a_{22} = \max_{-\pi/50 \le \phi(k) \le \pi/50} \frac{\sin\phi(k)}{\phi(k)} = 1 \tag{22}$$

$$M_{21}(z_2(k)) = \frac{a_{22} - z_2(k)}{a_{22} - a_{21}}, \qquad M_{22}(z_2(k)) = \frac{z_2(k) - a_{21}}{a_{22} - a_{21}} \tag{23}$$

Next, the overall switching T-S fuzzy model of TWMR is summarized as follows.

Region rule s: If $\phi(k) \in \mathbf{S}_s$, then

Local Plant rule si: If z_s is $M_{si}(z_s(k))$, then $\mathbf{X}(k+1) = \mathbf{A}_{si}\mathbf{X}(k) + \mathbf{B}_{si}\mathbf{u}(k)$

where $s = 1, 2, 3$; $i = 1, 2$. $\mathbf{A}_{11} = \mathbf{A}_{12} = \mathbf{A}_{31} = \mathbf{A}_{32} = \begin{bmatrix} 1 & 0 \\ 0 & 1 \end{bmatrix}$, $\mathbf{A}_{21} = \begin{bmatrix} 1 & C \cdot a_{21} \cdot \Delta t \\ 0 & 1 \end{bmatrix}$, $\mathbf{A}_{22} = \begin{bmatrix} 1 & C \cdot a_{22} \cdot \Delta t \\ 0 & 1 \end{bmatrix}$, $\mathbf{B}_1 = \begin{bmatrix} 1 & 0 \\ 0 & 1 \end{bmatrix} \Delta t$, $\mathbf{B}_{11} = \begin{bmatrix} 1 & 0 \\ 0 & 1 \end{bmatrix} \Delta t$, $\mathbf{B}_{12} = \begin{bmatrix} 0.01 & 0 \\ 0 & 1 \end{bmatrix} \Delta t$, $\mathbf{B}_{21} = \mathbf{B}_{22} = \begin{bmatrix} 0 \\ 1 \end{bmatrix} \Delta t$, $\mathbf{B}_{31} = \begin{bmatrix} -0.01 & 0 \\ 0 & 1 \end{bmatrix} \Delta t$, $\mathbf{B}_{32} = \begin{bmatrix} -1 & 0 \\ 0 & 1 \end{bmatrix} \Delta t$, $C = 0.5$.

After defuzzification, the final output of the above system is

$$\mathbf{X}(k+1) = \sum_{s=1}^{3} \sum_{i=1}^{2} g_s(\phi(k)) w_{si}(z_s(k)) [\mathbf{A}_{si}\mathbf{X}(k) + \mathbf{B}_{si}\mathbf{u}(k)] \tag{24}$$

where $g_s(\phi(k)) = \begin{cases} 1 & \text{if } \phi(k) \in \mathbf{S}_s \\ 0 & \text{otherwise} \end{cases}$, $w_{si}(z_s(k)) = \dfrac{M_{si}(z_s(k))}{\sum_{i=1}^{2} M_{si}(z_s(k))}$, $s = 1, 2, 3$. The switching T-S fuzzy model of TWMR is derived.

3. Controller Synthesis for the Switching T-S Fuzzy System.

This section describes a controller design for the above switching T-S fuzzy model of TWMR.

3.1. Switching PDC fuzzy controller.

The switching PDC controller is presented as:

Region rule s: If $\phi(k) \in \mathbf{S}_s$, then

Local Plant rule sj: If z_s is $M_{si}(z_s(k))$, then $\mathbf{u}(k) = -\mathbf{F}_{sj}\mathbf{X}(k)$ (25)

where $s = 1, 2, 3$; $j = 1, 2$. Then, the final output of the switching fuzzy controller is

$$\mathbf{u}(k) = -\sum_{s=1}^{3} \sum_{j=1}^{2} g_s(\phi(k)) w_{sj}(z_s(k)) \mathbf{F}_{sj}\mathbf{X}(k) \tag{26}$$

By (24) and (26), the final output of the closed-loop switching fuzzy system is

$$\mathbf{X}(k+1) = \sum_{s=1}^{3} \sum_{i=1}^{2} \sum_{j=1}^{2} g_s(k) w_{si}(k) w_{sj}(k) [\mathbf{A}_{si} - \mathbf{B}_{si}\mathbf{F}_{sj}]\mathbf{X}(k) \tag{27}$$

According to the Lyapunov stability criterion and Lyapunov function $V(k) = \mathbf{X}^T(k)\mathbf{P}\mathbf{X}(k)$, the following theorem provides the stabilization conditions for the system (27).

Theorem 3.1. *The switching T-S fuzzy model of TWMR (24) can be stabilized by the switching PDC (26), if there exist matrices* $\mathbf{Q} > 0$ *and* $\mathbf{K}_{si}$ *such that*

$$\begin{bmatrix} \mathbf{Q} & (*) \\ \mathbf{A}_{si}\mathbf{Q} - \mathbf{B}_{si}\mathbf{K}_{si} & \mathbf{Q} \end{bmatrix} > 0, \quad s = 1, 2, 3; \quad i = 1, 2, \tag{28}$$

$$\begin{bmatrix} \mathbf{Q} & (*) \\ \tilde{\mathbf{G}}_{sij} & \mathbf{Q} \end{bmatrix} > 0, \quad s = 1, 2, 3; \quad 1 \le i < j \le 2, \tag{29}$$

where $\mathbf{Q} = \mathbf{P}^{-1}$, $\mathbf{K}_{si} = \mathbf{F}_{si}\mathbf{Q}$ *and* $\tilde{G}_{sij} = [(\mathbf{A}_{si}\mathbf{Q} - \mathbf{B}_{si}\mathbf{K}_{sj}) + (\mathbf{A}_{sj}\mathbf{Q} - \mathbf{B}_{sj}\mathbf{K}_{si})]/2$. *The asterisk indicates the transposed element for symmetric positions.*

Proof: See Appendix A.

Remark 3.1. *Theorem 3.1 provides a switching T-S fuzzy model-based control design method for TWMR. The control design procedures are simple and direct. The Lyapunov function* $V(k) = \mathbf{X}^T(k)\mathbf{Q}^{-1}\mathbf{X}(k)$ *and control gains* $\mathbf{F}_{si} = \mathbf{K}_{si}\mathbf{Q}^{-1}$ *can be solved efficiently by MATLAB LMI toolbox. However, while the control theory is applied to the developed TWMR, some practical limitations must be considered. Simulation results reveal that the*

control gains are too large, leading to saturation of the control inputs in practical experiments. Additionally, the control design might provide slow state responses. Therefore, acceptable control gains are obtained using the guaranteed cost fuzzy control method.

3.2. **Guaranteed cost fuzzy control design.** If a controller $\mathbf{u}(k)$ exists such that not only a fuzzy system is stable but also a considered cost function is satisfied, then $\mathbf{u}(k)$ is called the guaranteed cost control law for the T-S fuzzy system. The cost function is defined as

$$J = \sum_{k=0}^{\infty} \left[\mathbf{X}^T(k)\mathbf{W}\mathbf{X}(k) + \mathbf{u}^T(k)\mathbf{R}\mathbf{u}(k) \right], \tag{30}$$

where $\mathbf{W}$ and $\mathbf{R}$ are given positive definite matrices. The following theorem provides a guaranteed cost control law for the TWMR system (24).

Theorem 3.2. *Consider the TWMR system (24) and the cost function (30) with given positive definite matrices* $\mathbf{W}$ *and* $\mathbf{R}$. *The fuzzy controller (26) not only can stabilize the TWMR system (24) asymptotically but also ensure that the cost function (30) satisfies* $J \leq J_0 = \mathbf{X}^T(0)\mathbf{Q}^{-1}\mathbf{X}(0)$, *if there exist matrices* $\mathbf{Q} > 0$ *and* $\mathbf{K}$, *such that*

$$\begin{bmatrix} \mathbf{Q} & (*) & (*) & (*) \\ (\mathbf{A}_{si}\mathbf{Q} - \mathbf{B}_{si}\mathbf{K}_{si}) & \mathbf{Q} & 0 & 0 \\ \mathbf{Q} & 0 & \mathbf{W}^{-1} & 0 \\ \mathbf{K}_{si} & 0 & 0 & \mathbf{R}^{-1} \end{bmatrix} > 0, \quad s = 1,2,3; \quad i = 1,2. \tag{31}$$

$$\begin{bmatrix} \mathbf{Q} & (*) & (*) & (*) & (*) & (*) \\ \tilde{\mathbf{G}}_{sij} & \mathbf{Q} & 0 & 0 & 0 & 0 \\ \mathbf{Q} & 0 & \mathbf{W}^{-1} & 0 & 0 & 0 \\ \mathbf{K}_{si} & 0 & 0 & \mathbf{R}^{-1} & 0 & 0 \\ \mathbf{Q} & 0 & 0 & 0 & \mathbf{W}^{-1} & 0 \\ \mathbf{K}_{si} & 0 & 0 & 0 & 0 & \mathbf{R}^{-1} \end{bmatrix} > 0, \quad s = 1,2,3; \quad 1 \leq i < j \leq 2. \tag{32}$$

Proof: See Appendix B.

Remark 3.2. *Based on Theorem 3.2, the TWMR system (24) can be stabilized and the cost index (30) is considered simultaneously. Notably, fast state responses and proper control gains can be achieved by choosing proper matrices* $\mathbf{W}$ *and* $\mathbf{R}$ *for (30), respectively (describe in next section). Proper control gains do not cause saturation of the driver circuit of the developed TWMR. Then the control design can directly apply to the developed TWMR. Consequently, the theoretical control design conforms to practical circumstances of the developed TWMR.*

4. **Simulation and Experimental Results.** This section introduces illustrative examples that demonstrate the effectiveness of the T-S model-based control for the developed TWMR. Firstly, two examples are illustrated based on Theorem 3.1 and Theorem 3.2, respectively. Example 4.3 describes how to determine an appropriate cost function for Theorem 3.2. Finally, Example 4.4 presents the experimental results of the TWMR control based on the proposed control law.

Example 4.1. *Consider the derived switching T-S fuzzy system (shown in Section 2.3) for TWMR. According to Theorem 3.1, the positive definite matrix* $\mathbf{P} = \mathbf{Q}^{-1}$ *and the*

control gains $\mathbf{F}_{si} = \mathbf{K}_{si}\mathbf{Q}^{-1}$ *can be obtained as follows.*

$$\mathbf{P} = \begin{bmatrix} 0.3347 & 0.0228 \\ 0.0228 & 0.2120 \end{bmatrix};$$
$$\mathbf{F}_{11} = \begin{bmatrix} 10.0057 & 0.0004 \\ -0.2820 & 9.9923 \end{bmatrix}; \quad \mathbf{F}_{12} = \begin{bmatrix} 25.0316 & 0.0431 \\ 0.9356 & 10.0307 \end{bmatrix};$$
$$\mathbf{F}_{21} = \begin{bmatrix} 0.9766 & 10.0597 \end{bmatrix}; \quad \mathbf{F}_{22} = \begin{bmatrix} 10.9766 & 10.0596 \end{bmatrix};$$
$$\mathbf{F}_{31} = \begin{bmatrix} -25.0316 & -0.0431 \\ 0.9356 & 10.0307 \end{bmatrix}; \quad \mathbf{F}_{32} = \begin{bmatrix} -10.0057 & -0.0004 \\ -0.2820 & 9.9923 \end{bmatrix}.$$

Figure 5(a) and Figure 5(b) show the trajectory and state responses of the TWMR with initial condition $\mathbf{X}(0) = [-1 \;\; 1.571]^T$, respectively. In Figure 5(a), the block denotes the instant attitude of the TWMR. Notably, to avoid the complexity, the following simulation results show only partial instant attitudes of TWMR. Simulation results indicate that the control design based on Theorem 3.1 can stabilize TWMR. Figure 6 and Table 1 show the control signals. However, in Table 1, the maximum magnitude $|u_2(k)|$ of the control signals is 15.98, i.e., larger than the boundary value of the driver circuit for the developed TWMR. The limit of our practical driver circuit is 15. Next, Theorem 3.2 is considered to avoid the control signal being over the limit of the driver circuit.

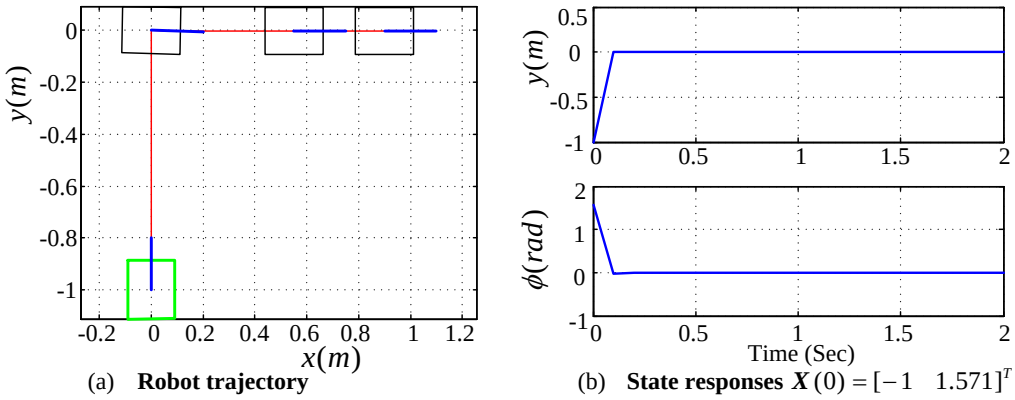

(a) **Robot trajectory** (b) **State responses** $\boldsymbol{X}(0) = [-1 \quad 1.571]^T$

FIGURE 5. Simulation results of Example 4.1

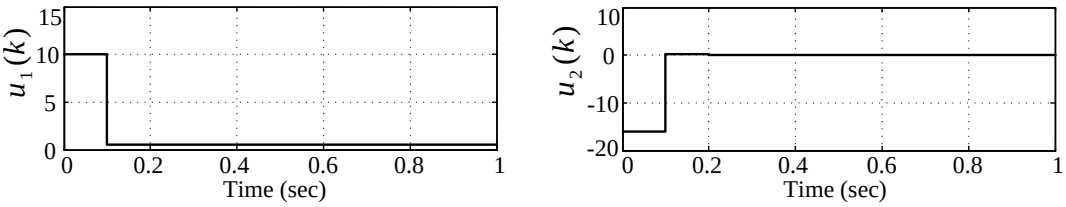

FIGURE 6. Control singles of Example 4.1

Example 4.2. *Consider the derived switching T-S fuzzy system (shown in Section 2.3) for TWMR. Using Theorem 3.2 and arbitrarily choosing* $\mathbf{W} = \mathbf{R} = diag(1, 1)$*, the positive*

TABLE 1. Significant control singles of Example 4.1

	$k=0$	$k=1$	$k=2$	$k=3$	$k=4$
$u_1(k)$	10.01	0.5	0.5	0.5	0.5
$u_2(k)$	-15.98	0.27	< 0.01	< 0.01	< 0.01

definite matrix $\mathbf{P} = \mathbf{Q}^{-1}$ *and the control gains* $\mathbf{F}_{si} = \mathbf{K}_{si}\mathbf{Q}^{-1}$ *are obtained as follows.*

$$\mathbf{P} = \begin{bmatrix} 1911 & 139.47 \\ 139.47 & 149.2 \end{bmatrix};$$

$$\mathbf{F}_{11} = \begin{bmatrix} 7.4145 & 0.2807 \\ 3.5007 & 5.0729 \end{bmatrix}; \quad \mathbf{F}_{12} = \begin{bmatrix} 1.8368 & 0.0389 \\ 4.7724 & 5.1252 \end{bmatrix};$$

$$\mathbf{F}_{21} = \begin{bmatrix} 4.4405 & 4.9616 \end{bmatrix}; \quad \mathbf{F}_{22} = \begin{bmatrix} 4.4400 & 4.9613 \end{bmatrix};$$

$$\mathbf{F}_{31} = \begin{bmatrix} -1.8368 & -0.0389 \\ 4.7724 & 5.1252 \end{bmatrix}; \quad \mathbf{F}_{32} = \begin{bmatrix} -7.4145 & -0.2807 \\ 3.5007 & 5.0729 \end{bmatrix}.$$

Figure 7(a) and Figure 7(b) show the trajectory and state responses of TWMR with the initial condition $\mathbf{X}(0) = [-1 \quad 1.571]^T$, respectively. Obviously, the TWMR is asymptotically stabilized. Figure 8 and Table 2 show the control signals. In Table 2, the maximum magnitude $|u_2(k)|$ of the control signals is 6.97, which is smaller than the boundary value of the driver circuit for the developed TWMR. Simulation results indicate that the control design based on Theorem 3.2 not only can stabilize the TWMR but also avoid triggering the saturation region of the driver circuit.

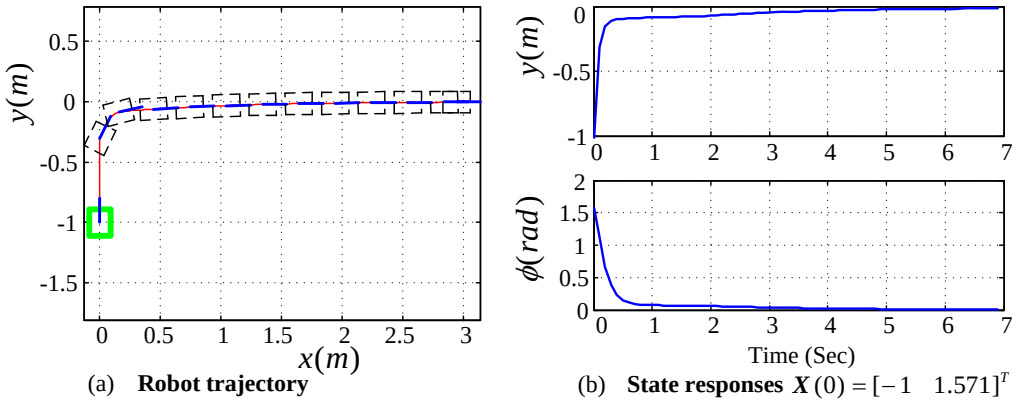

(a) **Robot trajectory** (b) **State responses** $\boldsymbol{X}(0) = [-1 \quad 1.571]^T$

FIGURE 7. Simulation results of Example 4.2

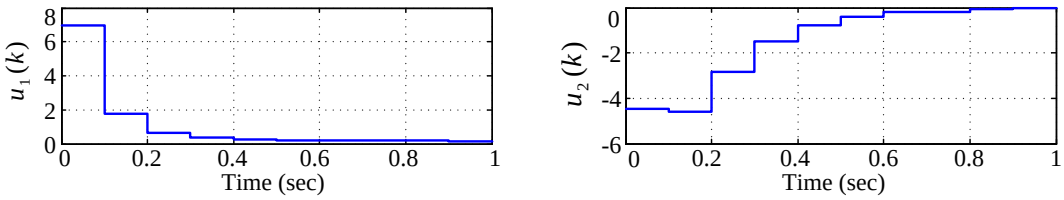

FIGURE 8. Control singles of Example 4.2

In Example 4.2, simulation results demonstrate the utility Theorem 3.2 by arbitrarily choosing $\mathbf{W} = \mathbf{R} = diag(1, 1)$. According to the cost function (30), matrices $\mathbf{W}$ and

TABLE 2. Significant control singles of Example 4.2

	$k=0$	$k=1$	$k=2$	$k=3$	$k=4$
$u_1(k)$	6.97	1.78	0.61	0.35	0.25
$u_2(k)$	−4.46	−4.61	−2.81	−1.50	−0.77

$\mathbf{R}$ are concerned with the state vector $\mathbf{X}(k)$ and input vector $\mathbf{u}(k)$, respectively. The following example illustrates how to choose the suitable matrices $\mathbf{W}$ and $\mathbf{R}$.

Example 4.3. *The derived switching T-S fuzzy system (shown in Section 2.3) is stabilized based on Theorem 3.2. In this example, various matrices* $\mathbf{W}$ *and* $\mathbf{R}$ *are examined to demonstrate how cost function influences state responses and control gains. Consider the initial state* $\mathbf{X}(0) = [1 \;\; 3.131]^T$. *First, fix* $\mathbf{W} = diag(1,1)$ *and test* $\mathbf{R} = diag(0.1, 0.1)$, $\mathbf{R} = diag(1,1)$ *and* $\mathbf{R} = diag(10,10)$. *According to Figure 9, various matrices* $\mathbf{R}$ *induce different control signals. Simulation results indicate that a large diagonal element of matrix* $\mathbf{R}$ *leads to a small control gain. While* $\mathbf{R} = diag(10,10)$, *the control signals* $|u_1(k)|$ *and* $|u_2(k)|$ *are always smaller than 15, which is the limit of the driver circuit.*

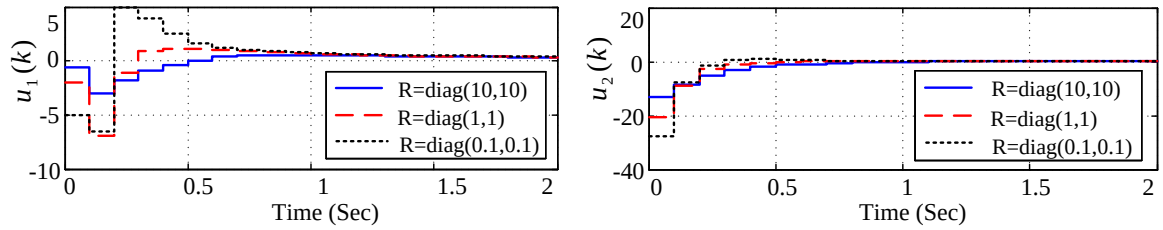

FIGURE 9. Comparison of control signals based on different $\mathbf{R}$

Second, fix $\mathbf{R} = diag(1,1)$ and test $\mathbf{W} = diag(0.1, 0.1)$, $\mathbf{W} = diag(1,1)$ and $\mathbf{W} = diag(10,10)$. According to Figure 10, various matrices $\mathbf{W}$ induce different control signals. Figure 10 indicates that a large element of matrix $\mathbf{W}$ leads to a small control gain.

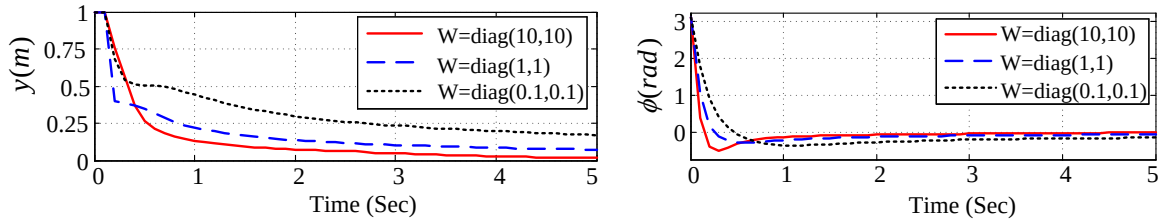

FIGURE 10. Comparison of control signals based on different $\mathbf{W}$

For the cost function (30), the diagonal terms of matrix $\mathbf{W}$ are the relative weights of the states $\mathbf{y}(k)$ and $\phi(k)$, respectively. Likewise, the diagonal terms of matrix $\mathbf{R}$ are relative weights of the states $\mathbf{u}_1(k)$ and $\mathbf{u}_2(k)$, respectively. The simulation results follow the above statements and also illustrate how to determine the scale of matrices $\mathbf{W}$ and $\mathbf{R}$. Based on the hardware constraints and performance requirements of the developed TWMR, $\mathbf{W} = diag(3,1)$ and $\mathbf{R} = diag(10,10)$ are determined for the following experiments.

Example 4.4. *In this example, Theorem 3.2 is applied to the developed TWMR. According to Example 4.3,* $\mathbf{W} = diag(3,1)$ *and* $\mathbf{R} = diag(10,10)$ *are determined for the*

cost function (30). Following (31) and (32), the designed controller can be obtained by MATLAB LMI toolbox. Figure 11 summarizes the experimental results with four different initial states $\mathbf{X}(0) = [-1 \quad 1.571]^T$, $\mathbf{X}(0) = [-1 \quad 3.131]^T$, $\mathbf{X}(0) = [-1 \quad 0.01]^T$ *and* $\mathbf{X}(0) = [1 \quad 0.01]^T$, *respectively. Figure 11 also compares the simulation and experimental trajectories. The block in the dashed line denotes the simulation trajectory based on the switching T-S fuzzy model of TWMR. Also, the block in the solid line denotes the experimental trajectory of the developed TWMR. Experimental and simulation trajectories always significantly differ from each other while TWMR turns its direction. We believe that the initial state and/or the friction with respect to the passive caster of the developed TWMR induces such differences. Despite the differences that exist in Figure 11, the experimental and simulation trajectories closely resemble each other. Figure 11 shows the effectiveness of the proposed guaranteed cost control law.*

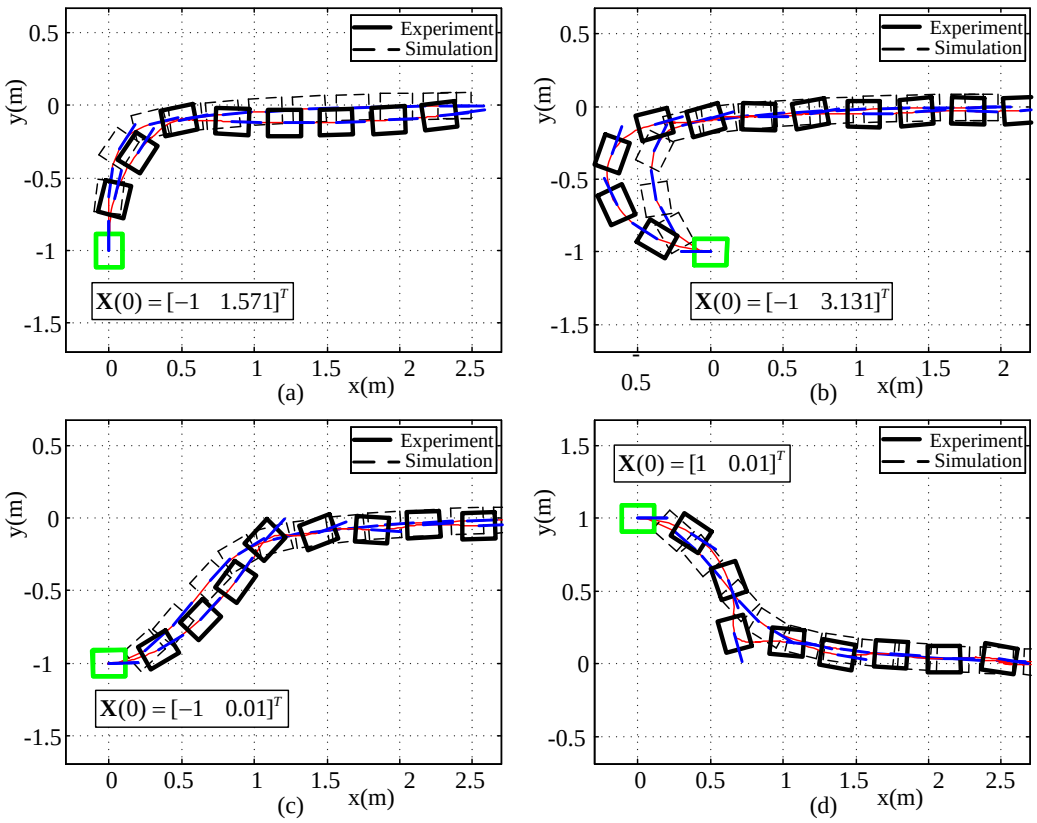

FIGURE 11. Comparison of experimental and simulation results

5. **Conclusions.** This work describes a developed TWMR and its switching T-S fuzzy model. A switching T-S model-based guaranteed cost control law is also developed for the position control of TWMR. By choosing a proper cost function for the guaranteed cost control design, Theorem 3.2 can provide an adequate control gain for the developed TWMR. The control gains can be effectively solved by Matlab LMI toolbox. Finally, experimental results demonstrate the effectiveness of the proposed method.

Acknowledgment. This work was supported by the National Science Council of Taiwan under the Grant NSC100-2221-E-032-006 and NSC100-2221-E-032-008. The authors also gratefully acknowledge the helpful comments and suggestions of the reviewers, which have improved the presentation.

REFERENCES

[1] J. Barraquand and J. C. Latombe, On nonholonomic mobile robots and optimal maneuvering, *Proc. of IEEE Int. Symp. Intell. Contr.*, pp.340-347, 1989.

[2] J. B. Coulaud, G. Campion, G. Bastin and M. De Wan, Stability analysis of a vision-based control design for an autonomous mobile robot, *IEEE Trans. Robot.*, vol.22, pp.1062-1069, 2006.

[3] Y. Ma, J. Kosecka and S. S. Sastry, Vision guided navigation for a nonholonomic mobile robot, *IEEE Trans. Robot. Automat.*, vol.15, pp.521-536, 1999.

[4] T. J. Ren, T. C. Chen and C. J. Chen, Motion control for a two-wheeled vehicle using a self-tuning PID controller, *Control Eng. Pract.*, vol.16, pp.365-375, 2008.

[5] D. Sun, G. Feng, C. M. Lam and H. N. Dong, Orientation control of a differential mobile robot through wheel synchronization, *IEEE/ASME Trans. Mechatron.*, vol.10, pp.345-351, 2005.

[6] G. Scaglia et al., A linear-interpolation-based controller design for trajectory tracking of mobile robots, *Control Eng. Pract.*, vol.18, pp.318-329, 2010.

[7] L. Jiang, M. Deng and A. Inoue, Obstacle avoidance and motion control of a two wheeled mobile robot using SVR technique, *International Journal of Innovative Computing, Information and Control*, vol.5, no.2, pp.253-262, 2009.

[8] Y. Zuo, Y. Wang, X. Liu, S. X. Yang, L. Huang, X. Wu and Z. Wang, Neural network robust control for a nonholonomic mobile robot including actuator dynamics, *International Journal of Innovative Computing, Information and Control*, vol.6, no.8, pp.3437-3449, 2010.

[9] B. S. Chen, C. S. Wu and H. J. Uang, A minimax tracking design for wheeled vehicles with trailer based on adaptive fuzzy elimination scheme, *IEEE Trans. Contr. Syst. Technol.*, vol.8, pp.418-434, 2000.

[10] T. Das and I. N. Kar, Design and implementation of an adaptive fuzzy logic-based controller for wheeled mobile robots, *IEEE Trans. Contr. Syst. Technol.*, vol.14, pp.501-510, 2006.

[11] T. H. Lee et al., A practical fuzzy logic controller for the path tracking of wheeled mobile robots, *IEEE Control Syst. Mag.*, vol.23, pp.60-65, 2003.

[12] F. M. Raimondi and M. Melluso, A new fuzzy robust dynamic controller for autonomous vehicles with nonholonomic constraints, *Robot. Auton. Syst.*, vol.52, pp.115-131, 2005.

[13] C. F. Juang and C. H. Hsu, Reinforcement ant optimized fuzzy controller for mobile-robot wall-following control, *IEEE Trans. Ind. Electron.*, vol.56, pp.3931-3940, 2009.

[14] Z. G. Hou et al., Adaptive control of an electrically driven nonholonomic mobile robot via backstepping and fuzzy approach, *IEEE Trans. Contr. Syst. Technol.*, vol.17, pp.803-815, 2009.

[15] K. Tanaka and H. O. Wang, *Fuzzy Control System Design and Analysis: A Linear Matrix Inequality Approach*, Wiley, New York, 2001.

[16] K. Tanaka, M. Iwasaki and H. O. Wang, Switching control of an R/C hovercraft: Stabilization and smooth switching, *IEEE Trans. Syst., Man, Cybern. B*, vol.31, pp.853-863, 2001.

[17] K. Tanaka, S. Hori and H. O. Wang, Multiobjective control of a vehicle with triple trailers, *IEEE/ASME Trans. Mechatron.*, vol.7, pp.357-368, 2002.

[18] H.-Y. Chu, K.-H. Tsai and W.-J. Chang, Fuzzy control of active queue management routers for transmission control protocol networks via time-delay affine Takagi-Sugeno fuzzy models, *International Journal of Innovative Computing, Information and Control*, vol.4, no.2, pp.291-312, 2008.

[19] H. Chung, S. Wu and W. Chang, Regional fuzzy control for nonlinear ship steering systems, *International Journal of Innovative Computing, Information and Control*, vol.4, no.7, pp.1635-1646, 2008.

[20] Y. J. Chen, W. J. Wang and C. L. Chang, Guaranteed cost control for an overhead crane with practical constraints: Fuzzy descriptor system approach, *Eng. Appl. Artif. Intell.*, vol.22, pp.639-645, 2009.

[21] K. H. Su, Y. Y. Chen and S. F. Su, Design of neural-fuzzy-based controller for two autonomously driven wheeled robot, *Neurocomputing*, vol.73, pp.2478-2488, 2010.

[22] D. J. Choi and P. G. Park, Guaranteed cost controller design for discrete-time switching fuzzy system, *IEEE Trans. Syst., Man, Cybern. B*, vol.34, pp.110-119, 2004.

[23] P. T. Lin, C. H. Wang and T. T. Lee, Time-optimal control of T-S fuzzy models via lie algrbra, *IEEE Trans. Fuzzy Syst.*, vol.17, pp.737-749, 2009.

Appendix A: Proof of Theorem 3.1. Consider a candidate of Lyapunov function $V(\mathbf{X}(k)) = \mathbf{X}^T(k)\mathbf{P}\mathbf{X}(k)$, $\mathbf{P} > 0$, for the closed-loop switching fuzzy system (24). Then,

$$
\begin{aligned}
&\Delta V(\mathbf{X}(k)) = V(\mathbf{X}(k+1)) - V(\mathbf{X}(k)) = \mathbf{X}^T(k+1)\mathbf{P}\mathbf{X}(k+1) - \mathbf{X}^T(k)\mathbf{P}\mathbf{X}(k) \\
&= \left(\sum_{s=1}^{3}\sum_{i=1}^{2}\sum_{j=1}^{2} g_s(k)w_{si}(k)w_{sj}(k)[\mathbf{A}_{si} - \mathbf{B}_{si}\mathbf{F}_{sj}]\mathbf{X}(k)\right)^T \cdot \mathbf{P} \\
&\quad \cdot \left(\sum_{s=1}^{3}\sum_{i=1}^{2}\sum_{j=1}^{2} g_s(k)w_{si}(k)w_{sj}(k)[\mathbf{A}_{si} - \mathbf{B}_{si}\mathbf{F}_{sj}]\mathbf{X}(k)\right) - \mathbf{X}^T(k)\mathbf{P}\mathbf{X}(k) \\
&\le \sum_{s=1}^{3}\sum_{i=1}^{2}\sum_{j=1}^{2} g_s(k)w_{si}(k)w_{sj}(k)\mathbf{X}^T(k)\left[\frac{(\mathbf{A}_{si} - \mathbf{B}_{si}\mathbf{F}_{sj}) + (\mathbf{A}_{sj} - \mathbf{B}_{sj}\mathbf{F}_{si})}{2}\right]^T \\
&\quad \cdot \mathbf{P}\left[\frac{(\mathbf{A}_{si} - \mathbf{B}_{si}\mathbf{F}_{sj}) + (\mathbf{A}_{sj} - \mathbf{B}_{sj}\mathbf{F}_{si})}{2}\right]\mathbf{X} - \mathbf{X}^T(k)\mathbf{P}\mathbf{X}(k) \\
&\le \sum_{s=1}^{3}\sum_{i=1}^{2} g_s(k)w_{si}^2(k)\mathbf{X}^T(k)\left[(\mathbf{A}_{si} - \mathbf{B}_{si}\mathbf{F}_{si})^T\mathbf{P}(\mathbf{A}_{si} - \mathbf{B}_{si}\mathbf{F}_{si}) - \mathbf{P}\right]\mathbf{X}(k) \\
&\quad +2\cdot\sum_{s=1}^{3}\sum_{i=1}^{2}\sum_{i<j} g_s(k)w_{si}(k)w_{sj}(k)\mathbf{X}^T(k)[\mathbf{G}_{sij}^T\mathbf{P}\mathbf{G}_{sij} - \mathbf{P}]\mathbf{X}(k) \qquad (33)
\end{aligned}
$$

where $\mathbf{G}_{sij} = [(\mathbf{A}_{si} - \mathbf{B}_{si}\mathbf{F}_{sj}) + (\mathbf{A}_{sj} - \mathbf{B}_{sj}\mathbf{F}_{si})]/2$. Then $\Delta V(k) < 0$, if

$$(\mathbf{A}_{si} - \mathbf{B}_{si}\mathbf{F}_{si})^T\mathbf{P}(\mathbf{A}_{si} - \mathbf{B}_{si}\mathbf{F}_{si}) - \mathbf{P} < 0, \quad s = 1,2,3; \quad i = 1,2; \qquad (34)$$

$$\mathbf{G}_{sij}^T\mathbf{P}\mathbf{G}_{sij} - \mathbf{P} < 0, \quad s = 1,2,3; \quad i \le i < j \le 2. \qquad (35)$$

By Lyapunov stability criterion, it implies the switching PDC fuzzy controller (26) can stabilize the TWMR system (24). By Schur complement, (34) and (35) are equivalent to following equations.

$$\begin{bmatrix} \mathbf{P} & (*) \\ \mathbf{A}_{si} - \mathbf{B}_{si}\mathbf{F}_{si} & \mathbf{P}^{-1} \end{bmatrix} > 0, \quad s = 1,2,3; \quad i = 1,2. \qquad (36)$$

$$\begin{bmatrix} \mathbf{P} & (*) \\ \mathbf{G}_{sij} & \mathbf{P}^{-1} \end{bmatrix} > 0, \quad s = 1,2,3; \quad 1 \le i < j \le 2. \qquad (37)$$

Multiplying both sides of the above inequalities by *block-diag*$[\mathbf{P}^{-1} \quad \mathbf{I}]$, then we can obtain (28) and (29). The proof of Theorem 3.1 is completed.

Appendix B: Proof of Theorem 3.2. Consider the Lyapunov function as Theorem 3.1. Apply the corresponding part of (33), then

$$
\begin{aligned}
&\Delta V(\mathbf{X}(k)) + \mathbf{X}^T(k)\mathbf{W}\mathbf{X}(k) + \mathbf{u}^T(k)\mathbf{R}\mathbf{u}(k) \\
&\le \mathbf{X}^T(k)\Bigg(\sum_{s=1}^{3}\sum_{i=1}^{2} g_s(k)w_{si}^2(k)\left[(\mathbf{A}_{si} - \mathbf{B}_{si}\mathbf{F}_{si})^T\mathbf{P}(\mathbf{A}_{si} - \mathbf{B}_{si}\mathbf{F}_{si}) - \mathbf{P} + \mathbf{W} + \mathbf{F}_{si}^T\mathbf{R}\mathbf{F}_{si}\right] \\
&\quad +2\cdot\sum_{s=1}^{3}\sum_{i=1}^{2}\sum_{i<j} g_s(k)w_{si}(k)w_{sj}(k)[\mathbf{G}_{sij}^T\mathbf{P}\mathbf{G}_{sij} - \mathbf{P} + 2\mathbf{W} + \mathbf{F}_{si}^T\mathbf{R}\mathbf{F}_{si} + \mathbf{F}_{sj}^T\mathbf{R}\mathbf{F}_{sj}]\Bigg)\mathbf{X}(k)
\end{aligned}
$$

If

$$(\mathbf{A}_{si} - \mathbf{B}_{si}\mathbf{F}_{si})^T\mathbf{P}(\mathbf{A}_{si} - \mathbf{B}_{si}\mathbf{F}_{si}) - \mathbf{P} + \mathbf{W} + \mathbf{F}_{si}^T\mathbf{R}\mathbf{F}_{si} < 0, \quad s = 1,2,3; \quad i = 1,2; \quad (38)$$

$$\mathbf{G}_{sij}^T\mathbf{P}\mathbf{G}_{sij} - \mathbf{P} + 2\mathbf{W} + \mathbf{F}_{si}^T\mathbf{R}\mathbf{F}_{si} + \mathbf{F}_{sj}^T\mathbf{R}\mathbf{F}_{sj} < 0, \quad s = 1,2,3; \quad i \le i < j \le 2 \quad (39)$$

then

$$\Delta V(\mathbf{X}(k)) + \mathbf{X}^T(k)\mathbf{W}\mathbf{X}(k) + \mathbf{u}^T(k)\mathbf{R}\mathbf{u}(k) < 0 \tag{40}$$

Summing (40) from $k = 0$ to $k = \infty$, then we have

$$\sum_{k=0}^{\infty}[\mathbf{X}^T(k)\mathbf{W}\mathbf{X}(k) + \mathbf{u}^T(k)\mathbf{R}\mathbf{u}(k)] < -\sum_{k=0}^{\infty}\Delta V(\mathbf{X}(k)) = V(\mathbf{X}(0)) - V(\mathbf{X}(\infty + 1))$$

Since $V(\mathbf{X}(k)) \leq 0$ and $\lim_{k\to\infty} V(\mathbf{X}(k)) = 0$. Hence,

$$J \leq J_0 = V(\mathbf{X}(0)) = \mathbf{X}^T(0)\mathbf{P}\mathbf{X}(0). \tag{41}$$

The rest proof procedures are similar to Appendix A. Equations (38) and (39) are equivalent to (31) and (30). The proof of Theorem 3.2 is completed.